energy&fuels

Article

pubs.acs.org/EF

# Tars from Fluidized Bed Gasification of Raw and Torrefied *Miscanthus* x *giganteus*

Alen Horvat,[†] Marzena Kwapinska,[*,‡] Gang Xue,[†] Luc P. L. M. Rabou,[∥] Daya Shankar Pandey,[†] Witold Kwapinski,[†,§] and James J. Leahy[†,§]

[†]Carbolea Research Group, Department of Chemical and Environmental Sciences, [‡]Technology Centre for Biorefining and Bioenergy, and [§]Materials & Surface Science Institute, University of Limerick, Limerick V94 T9PX, Ireland

[∥]Biomass & Energy Efficiency, Energy Research Centre of The Netherlands (ECN), 1755 Petten, Netherlands

**ABSTRACT:** The current study investigates the effect of temperature, equivalence ratio, and biomass composition on tar yields and composition. Torrefied and raw *Miscanthus* x *giganteus* (M×G) were used as biomass feedstocks in an atmospheric bubbling fluidized bed gasifier for experiments undertaken between 660 and 850 °C and equivalence ratios from 0.18 to 0.32. Tar was sampled according to the solid phase adsorption method and analyzed by gas chromatography. There is an indication that torrefied M×G produces higher amounts of total GC-detectable tar as well as higher yields of 20 individually quantified tar compounds compared with those of raw M×G. Under similar gasification conditions (800 °C and an equivalence ratio of 0.21), the total GC-detectable tar for torrefied M×G is approximately 42% higher than that for raw M×G. Higher tar yields are observed to be related to higher lignin and lower moisture content of torrefied M×G. The effect of temperature on tar yields is in good agreement with the literature. The highest yield of total GC-detectable tar, secondary tars, and tertiary-alkyl tars is observed between 750 and 800 °C, followed by a decrease at higher temperature, whereas tertiary-polycyclic aromatics increase with the temperature over the range tested. The effect of equivalence ratio on total GC-detectable tar is not clear because data points vary significantly (up to 47%) over the range of equivalence ratios tested. Temperature is the main driver for tar production and its chemical composition; however, this study indicates that tar yields depend significantly on biomass composition.

## 1. INTRODUCTION

Biomass gasification is an important component of biomass-based renewable energy systems. Via gasification, biomass can be utilized in combined heat and power production and for the production of intermediates for organic synthesis in various chemical industries. However, for most applications the product gas needs to be cleaned of impurities such as particulates, alkali metals, chlorine, sulfur, and tars. Tar is a black and sticky material potentially giving rise to system malfunction if condensation occurs; therefore, tar reduction/mitigation remains one of the biggest challenges in the commercialization of biomass-derived fuel gases.[1] The standardized guideline for tar measurement defines tar as a generic (unspecific) term for all organic compounds present in the gasification product gas excluding gaseous hydrocarbons (1−6 carbon atoms).[2]

Biomass gasification in bubbling fluidized beds is typically undertaken in the temperature range between 700 and 900 °C where drying, pyrolysis, combustion, and gasification reactions take place.[1] The reaction pathways and the amount of tar in the gas depend on process conditions (i.e., temperature, equivalence ratio, residence time, and partial pressure of reactants), bed material properties, reactor configuration, and biomass composition.[3−5]

### 1.1. Effect of Process Temperature on Tar Evolution.

Process temperature is consistently described in the literature as a dominant factor in tar evolution during biomass gasification.[3,4,6] Tar development initiates with depolymerization of ligno-cellulosic material at temperatures between 200 and 500 °C, generating oxygen-rich primary tars possessing mainly acid, aldehyde, and ketone functional groups. Secondary tars develop from primary tars by partially losing functional groups and increasing the aromatic molecular structures at temperatures above 500 °C, whereas at 800 °C, the tar molecules undergo rearrangement into tertiary tars by completing the condensation pathway resulting in purely aromatic species. Desirable permanent gases such as $H_2$, CO, $CH_4$, and unsaturated $C_2$−$C_4$ hydrocarbons are derived from temperature-driven tar decomposition/evolution.[4,5,7] Total GC-detectable tar production reaches a peak at 700−750 °C after which there is a steep decrease in concentration.[8,9]

The temperature not only affects the amount of tar but also its composition. Secondary tars such as toluene, xylene, and styrene decease steadily as temperature increases. Oxygen-containing phenol, cresols, and benzofuran decrease significantly with temperature and are almost entirely reformed at 800 °C. Substituted and heteroatomic tars reform at lower temperatures by losing OH and $CH_3$ groups. Tertiary tars including benzene and polycyclic aromatic hydrocarbons (PAHs) increase exponentially with increasing temperature because of promoted polymerization reactions.[8,10] For complete thermal conversion of PAHs under pyrolysis conditions, temperatures of at least 1200 °C with residence times up to 10 s are required.[11] According to Morgan and Kandiyoti,[12] who refer to unpublished work at Imperial College of London, with the addition of reactive gases such as steam, complete tar conversion can be achieved at 900−950 °C with a residence times of about 1 s. However, in the

**Received:** March 4, 2016
**Revised:** May 20, 2016
**Published:** May 31, 2016





DOI: 10.1021/acs.energyfuels.6b00532
*Energy Fuels* 2016, 30, 5693−5704

Table 1. Literature Overview of Equivalence Ratio Effect on Tar Yields from Bubbling Fluidized Bed Gasifiers

| gasification conditions | equivalence ratio effect on tar yields | ref |
|---|---|---|
| feed rate constant, ER adjustment by manipulation of $O_2$ and $N_2$ ratio, ER range 0.22−0.32 at 700 °C | Tar yields reported as $g_{tar}\ kg^{-1}_{biomass(db)}$. | 8 |
| | Total GC-detectable tar decreased by 30%. | |
| | Single-ring species decreased. | |
| | Oxygenated compounds decreased steeply. | |
| | 2,3,4-Ring aromatics increased. | |
| feed rate constant, ER adjustment mechanism not reported, ER range 0.15−0.35 at 800 °C and with secondary air injection | Tar yields reported as $g_{tar}\ m^{-3}$. | 16 |
| | Total GC-detectable tar decreased considerably. | |
| | Styrene and phenol decreased. | |
| | Toluene and indene yields were highest at ER of 0.25 followed by a decline. | |
| | Naphthalene yield significantly increased. | |
| ER adjustment by manipulation of feed rate, ER range 0.25−0.45 at 800 °C | Tar yields reported as $g_{tar}\ Nm^{-3}$. | 6 |
| | Total organic carbon of condensates decreased significantly. | |
| ER adjustment by manipulation of feed rate, ER range 0.25−0.35 at 800 °C | Tar yields reported as % of feed (as received). | 3 |
| | Gravimetric tar yields increased. | |
| ER adjustment by manipulation of feed rate, ER range 0.22−0.28 with increasing temperature from 750 to 950 °C | Tar yields reported as $mg_{tar}\ Nm^{-3}$. | 9 |
| | Total GC-detectable tar yield, GC undetectable tar, heterocyclic and light aromatics decreased. | |
| | Two- and three-ring aromatics remained constant. | |
| | Larger PAH species and tar dew point increased. | |

same review, pyrolysis tar/oil is shown to be reduced at 900 °C to as little as about 4 wt %. Nevertheless, the small remaining fraction of tar/oil may correspond to recalcitrant tertiary tars (naphthalene, anthracene, etc.), which is still unacceptable for some gasification applications.

**1.2. Effect of Equivalence Ratio on Tar Evolution.** The equivalence ratio (ER), defined as the ratio between the oxygen introduced into the gasifier and the oxygen needed for the complete stoichiometric combustion of the fuel, is also an important process parameter as higher ER values increase the $CO_2$ and reduce $H_2$ and CO contents in the product gas.[13] Fitzpatrick et al.[14] studied eugenol reforming under both pyrolysis and oxygen-rich conditions. High-molecular-weight PAHs were generated in the absence of oxygen, whereas in the presence of oxygen, PAH formation was inhibited by reactions between radical intermediates and oxygen. In contrast, Kinoshita et al.[8] suggested that higher ER stimulates the formation of higher molecular weight PAHs. Tar reforming by oxidation may be limited during gasification because tar competes with more reactive permanent gases for the oxygen.[15] Table 1 summarizes the findings of the effects of ER on the evolution of gasification tars. However, in some types of gasifiers the ER cannot be independently studied. For example, in industrial-scale autothermal rigs the temperature inherently increases by increasing the ER, in which case tar production is an effect of temperature rather than ER.

Tar reforming in the hot product gas can be described by following reactions:[5,15]

Thermal cracking:

$$pC_nH_x \rightarrow qC_mH_y + rH_2 \quad (1)$$

Steam reforming:

$$C_nH_x + nH_2O \rightarrow (n + x/2)H_2 + nCO \quad (2)$$

Dry reforming:

$$C_nH_x + nCO_2 \rightarrow (x/2)H_2 + 2nCO \quad (3)$$

Carbon formation:

$$C_nH_x \rightarrow nC + (x/2)H_2 \quad (4)$$

Hydrogenation:

$$C_nH_x + (2n - x/2)H_2 \rightarrow nCH_4 \quad (5)$$

Oxidation reaction:

$$C_nH_x + (x/4 + n)O_2 \rightarrow (x/2)H_2O + nCO_2 \quad (6)$$

**1.3. Effect of Composition of Lignocellulosic Feedstock on Tar Evolution.** Tar formation has been linked to biomass composition. Compositional differences in cellulose, hemicellulose, lignin, water content, ash content, and also feedstock particle size significantly affect tar formation during the pyrolysis step. Cellulose, hemicellulose, and lignin are the major components of biomass materials, and their content varies significantly with the type of biomass.[5,7] Cellulose consists primarily of D-glucose. Hemicellulose is a polysaccharide comprised of sugars, such as glucose, xylose, mannose, galactose, arabinose, and uronic acids, whereas lignin is a macrostructure composed of three different phenyl propane monomers, coniferyl alcohol (softwood), syringyl alcohol (hardwood), and coumaryl alcohol (grasses and agricultural crops) with cross-linking between the phenyl propane units.[5] The phenyl groups in lignin are logical precursors for phenol, which has been identified as a precursor for naphthalene and other PAHs.[9] Lignin gives rise to higher total GC-detectable tar and PAHs than does cellulose and hemicellulose.[5,10] However, smaller quantities of phenols and PAHs can also be formed from cellulose and hemicellulose.[5,14]

Increasing the partial pressure of steam promotes tar steam reforming and water−gas shift reactions, but the availability of heat determines the rate of endothermic steam reactions.[6] Paasen and Kiel[9] tested wood with moisture contents between 10 and 45 wt % and observed a reduction in both the amount of tar as well as in the tar dew point with increasing biomass moisture.

Several authors report tar cracking reactions promoted by the inorganic species present in biomass.[16,17] Particularly, the amount of alkali metals and earth alkali metals in the biomass



DOI: 10.1021/acs.energyfuels.6b00532
Energy Fuels 2016, 30, 5693−5704

such as K and Na have been reported to reduce the yields of pyrolysis bio oils.[18]

Intraparticle phenomena add complexity to the chemical reactions that govern tar concentration and composition.[7] In a bubbling fluidized bed, most of the biomass particles float on the bed surface as a result of their lower density compared to bed material such as olivine. Following devolatilization from the particles, the volatiles immediately enter the freeboard where oxygen-driven tar cracking is limited. Instead, volatiles convert into aromatic tars via secondary reaction pathways. According to the study by Mayerhofer et al.,[19] only a low tar concentration was measured in the dense phase (silica sand) of the fluidized bed. The tar released in the bed seemed to be converted into dry gases (i.e., $CH_4$, CO, $CO_2$, and $H_2$) in the presence of the hot bed material. However, larger particles enable longer residence time for tars within the particle, which results in tar cracking and additional char formation as a consequence of tar carbonization. In contrast, the accelerated thermal conductivity through the smaller particles forces the diffusion of the volatiles outward.[12] Link et al.[17] studied the effect of biomass particle surface area and observed a pronounced tar reduction with higher surface area. They explained this phenomenon by tar readsorption on the porous char particles, resulting in an extended residence time of the tar within the particle. Moreover, the amount of char in the fluidized bed may play an important role in tar yields. Abu El-Rub et al.[20] investigated char and olivine tar cracking activity in a packed bed. High phenol and naphthalene conversion was observed in the char bed between 700 and 900 °C.

**1.4. Effect of Torrefaction Process on Tar Evolution.** Torrefaction is a slow pyrolysis process carried out between 220−300 °C, during which hemicellulose and cellulose slowly break down and lignin remains relatively intact. Torrefaction upgrades biomass properties by increasing the energy density, improving storage stability, and making it easier to feed into reactor.[21]

With respect to tars from gasification, torrefied biomass was reported to reduce tar formation as a consequence of the partial removal of volatiles during the torrefaction process.[22] Meng et al.[23] and Boateng and Mullen[24] compared the product distribution of nontorrefied and torrefied pine chips, hardwood, and switchgrass from fluidized bed pyrolysis. They concluded that with an increasing degree of torrefaction, the mass fraction and oxygen content of the pyrolysis oil decreased, whereas the yield of biochar and gas increased. The amounts of lignin derived products (i.e., phenols) and anhydrosugars increased with the severity of torrefaction whereas light acids, ketones, alcohols, and aldehydes decreased. Berrueco et al.[4] measured total GC-detectable tar from pressurized bubbling fluidized bed comparing torrefied spruce and torrefied forest residue. They found that when using sand as the bed material tar production varied from 65 to 80 g $kg^{-1}_{dry\ biomass}$ whereas when using dolomite yields were between 10 and 70 g $kg^{-1}_{dry\ biomass}$.

**1.5. Effect of Bed Material on Tar Evolution.** Olivine is used as a bed material in fluidized bed gasification experiments because of its high attrition resistance[25] helping to mitigate agglomeration problems and as a promoter of tar cracking reactions. Olivine consists mainly of silicon dioxide ($SiO_2$ 39−42 wt %), magnesium oxide (MgO 48−50 wt %), and iron(III) oxide ($Fe_2O_3$ 8−10 wt %) embedded in a tetrahedral silicate structure. $Fe_2O_3$ and metallic Fe are catalytically active in C−C and C−H bond dissociation reactions.[26,27] With respect to the reference bed material (i.e., silica sand), a significant reduction in tar (>70%), accompanied by an increase in gas yield, $H_2$, CO, and $CO_2$ is reported in the literature.[26,28,29]

The goal of this paper is to compare tar evolution over a set of gasification parameters during bubbling fluidized bed gasification of raw and torrefied M×G. To our knowledge, total GC-detectable tars from raw and torrefied biomass using BFB gasification have not been reported.

## 2. MATERIALS AND METHODS

Prior to gasification, *Miscanthus* x *giganteus* (M×G) pellets were crushed and torrefied according to a procedure described previously.[30] Torrefaction was conducted in small batch reactors packed with ∼1.3 kg of raw M×G, with the potential for some batch-to-batch variation. Consequently, all batches were combined and milled in a ball mill prior to characterization and testing to ensure homogeneity of the biomass. Gasification experiments were conducted at the Energy Research Centre of The Netherlands (ECN) using an externally heated laboratory-scale air-blown bubbling fluidized bed gasifier described elsewhere.[9] External heating enables variation of the ER independent of temperature. Adjustment of the air flow fixed the ER, whereas a supplementary stream of pure nitrogen was used to maintain similar initial fluidization conditions during all experiments. The gasification temperature was achieved using two external furnaces. For each experimental day, the gasifier was loaded with uncalcined olivine and heated to a set point 50 °C lower than the desired gasification temperature before feeding commenced. Typically, 2−4 different gasification conditions were tested during each experimental day without discharging the bed between experimental conditions. Experiments were conducted during two separate experimental campaigns, while attempting to keep operation procedures of both campaigns comparable. ECN Pt-1 and ECN Pt-2 were undertaken in 2013 and 2014, respectively. The gases were tested for tar by taking duplicate solid-phase adsorption (SPA) samples at 5 min intervals for each set of gasification conditions once steady state was reached. Selected information concerning the gasification process conditions is presented in Table 2 with additional details regarding the gasification experiments available elsewhere.[31]

A detailed description of SPA cartridge preparation, sampling, extraction, and chromatographic analysis is described elsewhere.[32] Briefly, SPA cartridges were filled with 500 mg of aminopropyl silica sorbent. A stainless-steel needle with the plastic cap was attached to one

**Table 2. Process Condition during Experimental Campaigns at ECN**

| ER | temperature (°C) | residence time in the free board (s) | ER | temperature (°C) | residence time in the free board (s) |
|---|---|---|---|---|---|
| Raw *Miscanthus* x *giganteus* | | | | | |
| 0.21[b] | 715 | 5.9 | 0.22[b] | 800 | 5.7 |
| 0.22[b] | 800 | 5.7 | 0.25[b] | 800 | 5.8 |
| 0.23[b] | 850 | 5.6 | 0.27[b] | 800 | 5.8 |
| | | | 0.30[b] | 800 | 5.8 |
| | | | 0.31[b] | 800 | 5.5 |
| | | | 0.32[a] | 800 | 5.6 |
| Torrefied *Miscanthus* x *giganteus* | | | | | |
| 0.20[a] | 660 | 6.4 | 0.18[a] | 800 | 5.1 |
| 0.20[a] | 700 | 5.6 | 0.21[a] | 800 | 5.0 |
| 0.20[a] | 750 | 5.4 | 0.22[b] | 800 | 5.2 |
| 0.21[a] | 800 | 5.0 | 0.23[b] | 800 | 5.2 |
| 0.20[a] | 850 | 4.6 | 0.23[a] | 800 | 5.3 |
| | | | 0.26[a] | 800 | 5.2 |
| | | | 0.26[b] | 800 | 5.2 |
| | | | 0.27[b] | 800 | 5.2 |
| | | | 0.28[b] | 800 | 5.0 |

[a]ECN Pt-1. [b]ECN Pt-2.



DOI: 10.1021/acs.energyfuels.6b00532
Energy Fuels 2016, 30, 5693−5704

end, and a conical rubber stopper sealed the other end of the SPA cartridge. Then, 100 mL of product gas was withdrawn from sampling port which was maintained at 400 °C.

Subsequently, the tar compounds were extracted from the sorbent but not later than 2 h after the sampling by the addition of 3 × 600 $\mu$L of dichloromethane. Naphtalene-$d_8$ and phenol-$d_6$ were added to the tar solutions as internal standards. Calibration curves prepared using known concentrations of naphthalene/naphtalene-$d_8$ and phenol/phenol-$d_6$ were applied for integration of the aromatic and phenolic tars, respectively.

An Agilent 7890A GC coupled with a triple-axis MSD 5975C was used for the separation and analysis of the tar solutions. A constant helium flow of 1.2 mL min$^{-1}$ was passed through a nonpolar HP-5MS capillary column (30 m × 0.25 mm, 0.25 $\mu$m film thickness). The injection port operated at 300 °C, and the oven temperature program was initiated at 30 °C for 5 min, before heating to 180 °C at 5 °C min$^{-1}$ and finally from 180 to 300 °C at 8 °C min$^{-1}$. The MSD operated in electron ionization mode at an ionization energy of 70 eV and full scan mode in the mass range 50−550 $m/z$. The transfer line, MSD ion source, and MSD quadrupole mass analyzer temperatures were maintained at 300, 220, and 200 °C, respectively.

## 3. RESULTS AND DISCUSSION

The data presented in Table 3 report the effect of torrefaction on the compositional changes of M×G in terms of proximate and ultimate properties as well as chemical composition of the lignocellulosic polymers. As expected on the basis of previous experience with torrefied M×G, moisture content and volatile matter are reduced by 70 and 10%, respectively.[30] The ash content increased by 50% and fixed carbon is doubled when compared to those of raw M×G. Apparent differences are observed in lignocellulosic composition between the torrefied and raw M×G. The hemicellulose content is reduced by 67% during torrefaction, whereas about 7% of cellulose was decomposed compared to raw M×G. As a result of drying as well as hemicellulose and cellulose decomposition, the initial mass of raw M×G is reduced on average by about 24%, resulting in a relative doubling of the amount of lignin on a dry and ash-free basis (daf).

**Table 3. Properties of Raw and Torrefied M×G[31]**

| proximate analysis (as received) (wt %) | raw | torrefied |
|---|---|---|
| moisture | 8.8 | 2.4 |
| volatile matter | 77.8 | 69.5 |
| ash | 2.8 | 4.2 |
| fixed carbon | 10.7 | 23.9 |
| **ultimate analysis (as received) (wt %)** | **raw** | **torrefied** |
| N | 0.6 | 0.7 |
| C | 42.3 | 51.1 |
| H | 6.4 | 6.0 |
| S | <0.01 | <0.01 |
| Cl | 0.2 | 0.2 |
| O (by difference) | 39.0 | 35.4 |
| **chemical composition (dry basis) (wt %)** | **raw** | **torrefied** |
| hemicellulose | 21.3 | 7.1 |
| cellulose | 42.8 | 39.8 |
| lignin | 21.3 | 42.8 |
| extractives | 4.7 | 4.7 |
| **chemical composition (dry and ash free basis) (wt %)** | **raw** | **torrefied** |
| hemicellulose | 22.3 | 7.3 |
| cellulose | 44.8 | 41.4 |
| lignin | 22.3 | 44.5 |
| extractives | 4.9 | 4.9 |

Figure 1 shows the particle size distribution of raw and torrefied M×G. The torrefied feedstock contains a larger fraction of fine particles, resulting in a mean particle diameter of 718 $\mu$m as compared to 1307 $\mu$m for the raw M×G. Torrefied M×G is also more brittle, and its particle size is likely to have been further reduced in the feeding system.

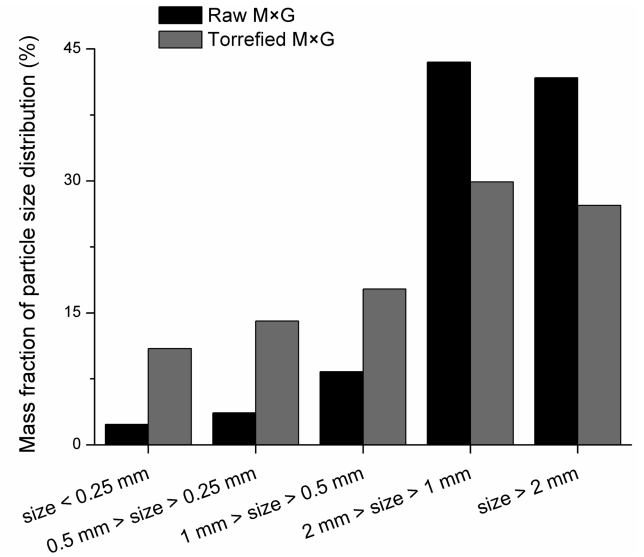


**Figure 1.** Particle size distribution of raw and torrefied M×G feed into gasification reactor.

Figure 2 compares the total ion current chromatograms of the tar compounds for torrefied and raw M×G. The chromatogram enables the detection of about 100 species; however, only 20 of the most abundant tars are identified using the NIST 08 MS library within MSD ChemStation. The identified tar compounds are presented in Table 4 in the order in which they eluted. Total GC-detectable tar in this paper includes tar molecules eluted from benzene ($M \approx 78$ amu) to benzo[$k$]fluoranthene ($M \approx 252$ amu). The results need to be viewed in a semiquantitative manner because the total GC-detectable tar was quantified by integration of the total ion current (TIC) chromatogram, whereas individual tar compounds were isolated and integrated in a selected-ion monitoring (SIM) chromatogram. The two different integration techniques introduce an uncertainty when the individual tar compounds are compared to the total GC-detectable tar quantities. When using the SPA method, measurement uncertainty may arise as a result of the different modes of integration, sampling efficiency, extraction recovery, and simplified quantitation methods (i.e., assuming the detector response is uniform for all compounds quantified) as previously addressed in by Ortiz et al.[33] and Horvat et al.[32] Therefore, direct comparison of tar values from a particular study such as this with other literature data needs to be undertaken with caution.

Tar yields are expressed on a mass basis as $g_{Tar}$ $kg^{-1}_{Biomass\text{-}daf}$ to eliminate any dilution effect in the product gas when the biomass feed rate is reduced or when the oxygen to nitrogen ratio is reduced to adjust for lower ER. This enables us to compare the differences in tar composition only related to torrefied and raw M×G.

The results of SPA tar in Figures 3−5 and 7−10 are presented in duplicate for each gasification condition to show the repeatability of the measurements and the random errors associated with fluctuations in the feeding rate. Table 5 shows



DOI: 10.1021/acs.energyfuels.6b00532
Energy Fuels 2016, 30, 5693−5704

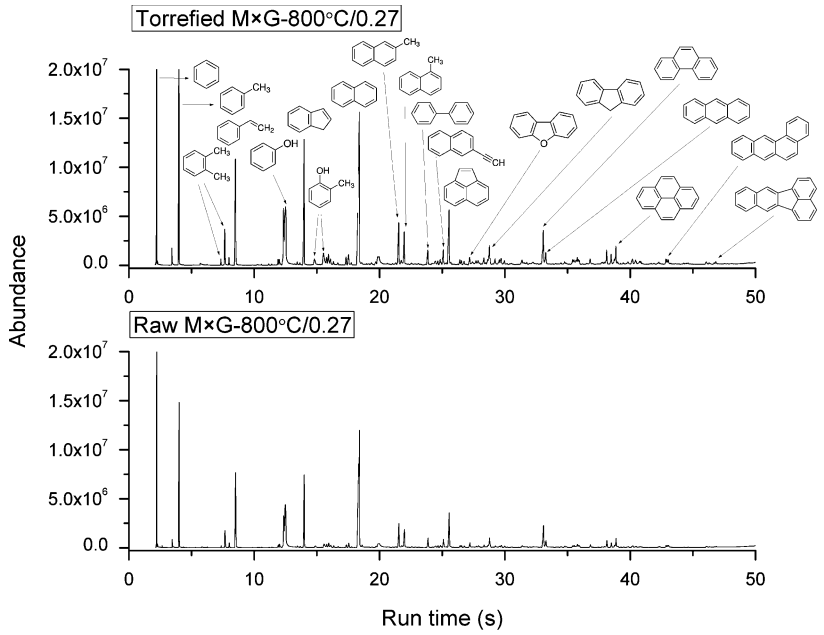


**Figure 2.** Total ion current chromatogram from GC-MS analysis, comparing tars from raw and torrefied M×G.

**Table 4. Identified Tar Compounds Together with the Retention Times and Classification According to Milne et al.[7]**

| tar compound | chromatographic retention time (min) | tar group |
|---|---|---|
| benzene | 2.19 | secondary |
| toluene | 3.96 | secondary |
| *o*/*m*/*p*-xylene | 7.66 + 8.55 | secondary |
| styrene | 8.51 | secondary |
| phenol | 12.54 | secondary |
| indene | 14.00 | secondary |
| *o*/*m*/*p*-cresol | 14.81 + 15.54 | secondary |
| naphthalene | 18.40 | tertiary-PAH |
| 2-methyl-naphthalene | 21.54 | tertiary-alkyl |
| 1-methyl-naphthalene | 21.98 | tertiary-alkyl |
| biphenyl | 23.86 | tertiary-alkyl |
| 2-ethenyl-naphthalene | 25.09 | tertiary-alkyl |
| acenaphthylene | 25.56 | tertiary-PAH |
| dibenzofuran | 27.20 | secondary |
| fluorene | 28.77 | tertiary-PAH |
| phenanthrene | 33.08 | tertiary-PAH |
| anthracene | 33.27 | tertiary-PAH |
| pyrene | 38.87 | tertiary-PAH |
| benz[*a*]anthracene | 42.94 | tertiary-PAH |
| benzo[*k*]fluoranthene | 46.831 | tertiary-PAH |

**Table 5. Measurement Repeatability of Total Gc Detectable Tar, Phenol, and Naphthalene Calculated for Each Experimental Campaign[a]**

| | total GC-detectable tar | phenol | naphthalene |
|---|---|---|---|
| ECN Pt.I | 9 | 11 | 15 |
| ECN Pt.II | 13 | 11 | 9 |

[a]Repeatability is expressed in (%).

the measurement repeatability of total GC-detectable tar, phenol, and naphthalene. Repeatability is calculated for both experimental campaigns independently and includes all conducted GC injections. The repeatability calculation spread sheet is adopted from TAPPI standard T 1200 and is available on the web (www.tappi.org/content/pdf/standards/useful.xls). The presented chromatographic repeatabilities are slightly higher than those reported in the relevant literature. Israelsson et al.[34] reported a relative standard deviation (RSD) within 10% for most of the tar compounds, whereas Ortiz et al.[33] reported chromatographic repeatability of 4 and 2% RSD for naphthalene and phenol, respectively. However, for the purpose of the current comparative study ,the measurement repeatability is considered acceptable.

**3.1. Effect of Temperature on Tar Yield and Composition.** Figure 3 shows the changes in the total, secondary, tertiary alkyl, and tertiary PAH tar groups generated from the raw and torrefied M×G as a function of gasification temperature. The main indication from Figure 3 is that torrefied M×G generates more total GC-detectable tar than does raw M×G. For the temperature range studied, the total GC-

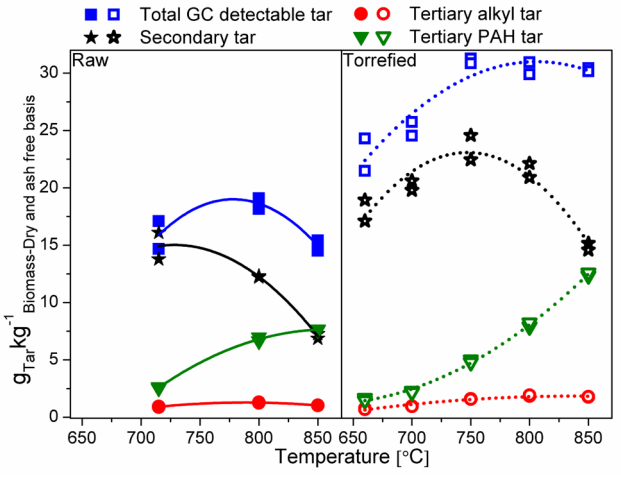


**Figure 3.** Temperature profile of the total GC-detectable tar, secondary, tertiary alkyl, and tertiary PAH tar groups at an equivalence ratio of 0.21 ± 0.02. Solid symbols, raw M×G; open symbols, torrefied M×G.



DOI: 10.1021/acs.energyfuels.6b00532
*Energy Fuels* 2016, 30, 5693−5704

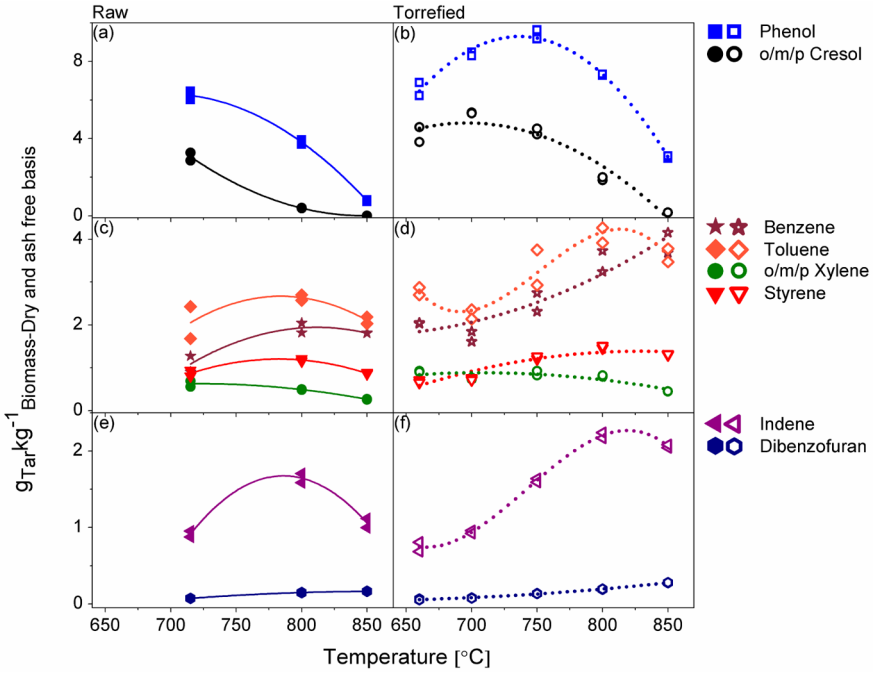


**Figure 4.** Temperature profile of the phenolic, single-ring aromatic, and two-ring aromatic tars from the secondary tar group at an equivalence ratio of 0.21 ± 0.02. Solid symbols, raw M×G; open symbols, torrefied M×G.

detectable tar produced from raw M×G accounts for ~1.6 wt % of the initial daf feedstock, whereas for torrefied M×G, it was around ~2.5 wt %. Under similar temperature conditions (800 °C), total GC-detectable tar for torrefied M×G is about 40% higher (30.4 versus 18.6 $g_{Total\ GC\text{-}detectable\ tar}\ kg^{-1}_{Biomass\text{-}daf}$). This indication is in contrast to Chen et al.[22] who suggested that torrefaction may reduce tar production. The lignocellulosic composition of the feedstock together with the water content seem to play the major roles in tar evolution. Torrefied M×G has about double lignin content (Table 3), which is a precursor for the aromatic species found in tar.[9] However, higher moisture content in raw biomass (Table 3) and product gas (see ref 31) enable higher rates of the tar steam reforming reaction (eq 2), particularly at gasification temperatures above 800 °C.

The peak production of total GC-detectable tar is observed for both feedstocks between 750 and 800 °C, which is in line with the trends observed for other feedstocks.[8,9] For torrefied M×G, the total GC-detectable tar did not decrease significantly after its peak production at 750 °C, which can be attributed to (1) decomposition of some heavy GC undetectable tar into the GC-detectable tar fraction due to thermal tar cracking,[9,35] (2) higher thermal stability of light PAHs due to the higher content of aromatic lignin in torrefied M×G[7] resulting in higher total GC-detectable tar yield, and (3) limited steam reforming of tars due to lower water content in the product gas derived from torrefied M×G.

Despite the higher ash content (4.2 vs 2.8 wt % as-received basis), torrefied M×G generates a higher tar quantity. Link et al.[17] observed a similar trend which indicates that the ash content in the biomass is not a determining factor during tar evolution. Higher ash content in the biomass particles did not give rise to any observable tar reduction because the residence time of tar vapors in the particles was significantly shorter than in the gas phase.

The residence times of the gas phase in the reactor were similar across all gasification conditions (Table 2), so the difference in the particle size between feedstock seems to be more important. Shorter residence time of volatiles within smaller torrefied particles as a result of faster diffusion of the tar vapors from small particles could contribute to higher tar yields for torrefied M×G.[36]

The yield of secondary tar species from torrefied M×G is significantly higher than from raw biomass, an indication that is consistent with previous reports by Fitzpatrick et al.[14] and Meng et al.,[23] who concluded that higher lignin content is directly responsible for high levels of oxygenated aromatics such as phenols, which are the main constituents of secondary tars. Secondary tars are the dominant species among the three tar groups at temperatures up to 850 °C, but above 850 °C, tertiary PAH tars seemed to predominate. Secondary tars derived from torrefied M×G show the highest concentrations at 750 °C, whereas secondary tars from raw M×G decrease in the temperature range from 715 to 850 °C. However, there is a reasonable possibility that a similar trend line would be observed for the secondary tars from both feedstock if additional gasification temperature between 650 and 750 °C were also be tested for raw M×G.

Tertiary-alkyl tars are not quantitatively significant. The concentration of tertiary-alkyl tars from raw M×G appears to peak at 800 °C followed by a gradual decrease, whereas torrefied tertiary-alkyl tars increase with temperature. Milne and Evans[7] observed peak production of tertiary-alkyl tars between 850 and 900 °C. Tars belonging to the tertiary-PAH tar group increase with gasification temperature for both feedstocks. Tertiary-PAH tars concentrations are about 8 times higher at 850 °C than at 650 °C, which is in agreement with Rabou et al.[10] who also used olivine as the bed material. We note that at 700 °C there is no difference in the yield of tertiary-PAHs between torrefied and raw M×G whereas at 850 °C torrefied M×G produces double the yield of tertiary-PAHs compared to the raw biomass suggesting significant reforming of phenols into PAHs. At high temperatures of 850 °C, the endothermic steam reforming reactions are


DOI: 10.1021/acs.energyfuels.6b00532
Energy Fuels 2016, 30, 5693−5704

promoted,[6] which leads to the lower formation of PAHs from the raw M×G where higher amounts of water were present in the product gas (see ref 31). In contrast, for torrefied M×G steam reforming reactions were limited as a result of lower contents of water in the product gas.

The trends for permanent gas production are similar for both raw and torrefied M×G (Figure 6a,b). An increase of $H_2$ and CO with temperature observed for both biomasses can partially be explained by the decrease of tar arising from dealkylation reactions,[4] whereas the observed consumption of $CO_2$ is likely to arise as a consequence of dry reforming of tar.[26]

The evolution of phenolic, single-ring aromatic, and two-ring aromatic tar compounds belonging to the secondary tar group as a function of temperature is presented in Figure 4. At about 700 °C, torrefied biomass generates 22−30% more phenols and 38−47% more cresols because of its higher lignin content, the main source of phenolic tars.[9] At temperatures up to 800 °C, the most abundant tar compounds within the group are phenols and cresols (68−33%), but above 800 °C, almost complete conversion of phenols and cresols occurs particularly for raw M×G. Phenol yield from the torrefied M×G remains relatively high at 850 °C as a result of the higher initial content of phenol in the tar.

The behavior observed for phenol closely follows that of the group of secondary tars (see Figures 3 and 4a,b), making phenol a good indicator of the evolution of secondary tar group. According to Dufour et al.[37] cresol reforms into phenol and toluene by demethylation and dehydration reactions with phenol, undergoing further conversion to benzene through dehydration. Fitzpatrick et al.[14] reported that phenols derived from lignin eliminate carbon monoxide to give the cyclopentadiene radical and its methyl derivatives, which are mainly converted in a reducing environment into benzene, toluene, indene, and naphthalene. Increased yields of CO (see Figure 6a) with temperature as well as increasing yields of benzene and toluene are observed for both feedstocks, which may indicate cracking of the abundant phenolic species.

Changes in aromatic secondary tars with temperature are presented in Figure 4c−f. The highest yields of toluene, styrene, and indene are observed at 800 °C for both feedstock. For both feedstock, *o*-/*m*-/*p*-xylene gradually decrease, whereas dibenzofuran steadily increase with the temperature. In the case of raw M×G, benzene formation appears to peak at 800 °C, whereas it increases continuously up to 850 °C in the case of the torrefied feedstock. Relatively abundant benzene indicates a significant degree of tar reforming.[11,36] However, the decrease of benzene, toluene, styrene, and indene at 850 °C is more evident in the case of raw M×G, which is probably due to the enhanced steam reforming reactions as mentioned earlier. It should be noted that benzene and toluene measurements shows poor repeatability making comparisons difficult. Moreover, during optimization of the SPA protocol, it was observed that both toluene and particularly benzene broke through the amino phase sorbent introducing sampling error, suggesting that underestimation of light tar compounds needs to be considered when using the SPA sampling method. The issue regarding inadequate sampling of benzene and toluene was reported previously by Ortiz el al.[38] and Horvat et al.[32]

Similar trends for secondary tar aromatics (one- and two-ring) were observed for other feedstock by Paasen and Kiel[9] and Dufour et al.[37] who suggested that indene reforms to either benzene or naphthalene at temperatures between 800 and 900 °C. Toluene likewise forms from cresols by dehydration and further converts to benzene by demethylation.

Similar trends are observed for both biomass feedstock for the evolution of individual tertiary-alkyl tar compounds with temperature, as presented in Figure 5a,b. The most abundant of the tertiary-alkyl tar molecules is 2-methyl-naphthalene, but quantitatively it is less significant since the yield is an order of magnitude lower than the most abundant tars, naphthalene, and phenol. The highest concentrations of alkylated naphthalenes is at 800 °C, but these decrease significantly at 850 °C, suggesting that they lose their alkyl groups and probably convert to naphthalene.[37] According to Fitzpatrick et al.,[14] methyl-naphthalenes are derivatives of methyl-cyclopentadienes. Biphenyl increased constantly with temperature. Paasen and Kiel[9] observed a similar trend for biphenyl, and they suggested that the growth mechanism of biphenyl operates via recombination of two phenyl radicals. Berrueco et al.[4] observed an increase of alkylated naphthalenes and biphenyl in the case of torrefied spruce, whereas for torrefied forest residue, a decrease was observed between 750 and 850 °C. They also suggested that alkylated naphthalenes and biphenyl may have a role as intermediate compounds in the polymerization pathways to higher molecular weight PAHs.

Figure 5c−f shows the evolution of individual tertiary-PAH tar compounds with temperature. For torrefied M×G, the trends for all eight PAHs were similar, showing exponential growth with increasing temperature. In the case of raw M×G, the growth rate of PAHs moderates above 800 °C, which again can be attributed to the enhanced steam reforming actions. Benzo(*k*)fluoranthrene arising from raw biomass appears to decrease at 850 °C; however, as a result of benzo(*a*)anthracene and benzo(*k*)fluoranthrene being well-below the limit of quantification by GC-MS,[32] the results need to be viewed with caution. Despite relatively low concentrations of the largest PAHs (i.e., <0.15 $g_{Tar\ compound}\ kg^{-1}_{Biomass\text{-}daf}$), the knowledge of their concentration is critical in terms of the ultimate exploitation of the product gas because they have a significant influence on the dew point of the product gas. For both biomass feedstock, naphthalene is the most abundant tar compound belonging to the tertiary-PAH tar group. The quantitative significance of naphthalene compared to the tertiary-PAH tar group decreases with temperature, suggesting that naphthalene is an intermediate in the reaction pathways to larger PAHs.[14] Naphthalene from torrefied M×G at the 660 °C makes up about 62% of the tertiary-PAH tar group, whereas at the 850 °C, the relative value decreases to about 53%. Relative values for the naphthalene from raw M×G decrease from 60 to 55% in the temperature range of 715−850 °C. Naphthalene can also be formed as a product of the cracking of higher molecular weight tars.[13] In contrast, the quantitative significance of naphthalene in relation to the total GC-detectable tar increased with the temperature, indicating tar conversion toward PAH compounds as temperature increases. The relative amount of naphthalene compared to the total GC-detectable tar increase from 10 to 30% and from 4 to 22% for raw and torrefied M×G, respectively. The increase of PAHs coincides with a decrease in phenols and methylated aromatics as a result of dealkylation, dehydration, decarbonylation, and polymerization reactions.[4]

With regard to permanent gases, methane (Figure 6a) yield was slightly higher for torrefied M×G and increases with the temperature, probably as a result of thermal cracking of aliphatic hydrocarbons[37] or as a result of ethane ($C_2H_6$) breaking down into the $CH_3^{\bullet}$ radicals that react with $H_2$ forming $CH_4$. This hypothesis is supported by the decreasing yields of $C_2H_6$



DOI: 10.1021/acs.energyfuels.6b00532
Energy Fuels 2016, 30, 5693−5704

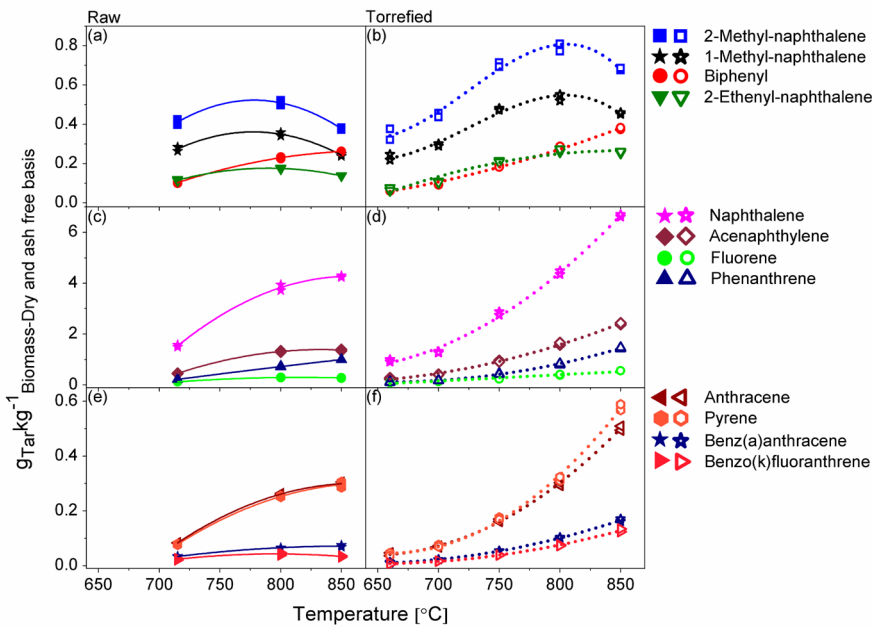


**Figure 5.** Temperature profile of the alkylated aromatic and PAH tars from the tertiary alkyl tar group at an equivalence ratio of 0.21 ± 0.02. Solid symbols, raw M×G; open symbols, torrefied M×G.

reported in Figure 6b. The concentration of acetylene ($C_2H_2$) and ethylene ($C_2H_4$) increase with increasing gasification temperature for both biomasses as shown in the Figure 6b. Temperature-driven demethylation reactions of methylated tar species give rise to the $CH_2^{\bullet}$ radicals that recombine to $C_2H_4$ or $C_2H_2 + H_2$. Literature data on the evolution of $C_2$ species vary probably because of different reaction conditions applied. Brage et al.[39] investigated pyrolysis products from hardwood chips and related the presence of $C_2$ species in the gas phase to the cracking of large organic molecules. Dufour et al.[37] related a consumption of $C_2H_4$ to the formation of higher PAHs via cyclization reactions.

**3.2. Effect of Equivalence Ratio on Tar Yield and Composition.** The gasifier used in this study was externally heated and the temperature was maintained independent of the ER. In industrial-scale gasifiers, high temperature can only be achieved by having higher ER or the use of $O_2$-enriched air. Therefore, the results presented here need to be compared with the studies conducted under comparable gasification conditions.

Figure 7 compares total GC-detectable tar yields generated from raw and torrefied M×G as a function of ER at constant temperature (800 °C), showing the variation between the two experimental campaigns conducted during ECN Pt-1 and ECN Pt-2. Results indicate that torrefied M×G produces more total GC-detectable tar than the raw feedstock. Over the range of ER investigated, the total GC-detectable tar from raw M×G is between 1.5 and 2.6 wt %, whereas that from torrefied M×G varies between 2.1 and 4.0 wt % of initial daf feedstock. For comparison, the total GC-detectable tar at ERs of 0.22 and 0.27 is taken only from the ECN Pt-2 experimental campaign. The total GC-detectable tar yield of raw M×G at an ER of 0.22 is about 18 $g_{\text{Total GC-detectable tar}}\ kg^{-1}_{\text{Biomass-daf}}$, whereas torrefied M×G at an ER 0.22 produces 23 g, representing a relative difference of 22%. Comparison between total GC-detectable tar values for raw and torrefied M×G at an ER of 0.27 shows a relative difference of 33%. As mentioned earlier, such a difference could be attributed to the higher lignin content of torrefied M×G and higher moisture content in raw biomass.[9] The data (see Figures 7−10)

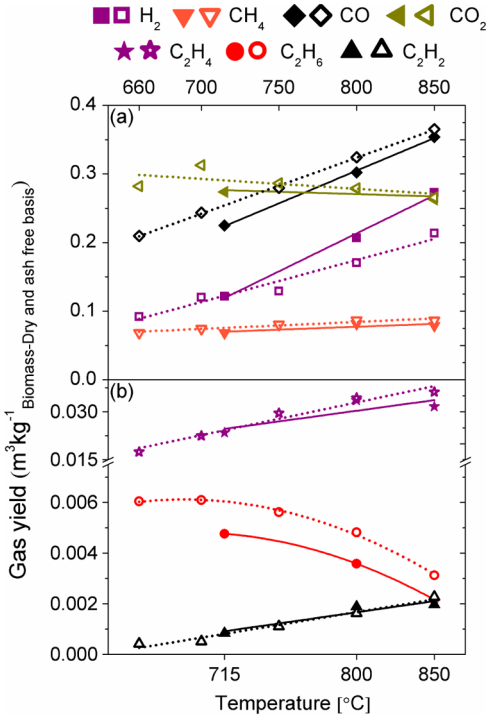


**Figure 6.** Gas composition as a function of gasification temperature at an equivalence ratio of 0.21 ± 0.02. Solid symbols and solid lines refer to raw M×G, whereas open symbols and dot lines refer to torrefied M×G.[31]

for the total and individual tar components as well as the permanent gas composition as a function of ER show no obvious trend, making it difficult to draw definitive conclusions regarding whether or not the ER influences tar production. Kinoshita et al.[8] and Hanping et al.,[16] using externally heated gasifiers and keeping the biomass feed rate constant, observed a decrease in tar with increasing ER. The explanation for not observing such a decline as ER increase is not clear, but possible reasons include



DOI: 10.1021/acs.energyfuels.6b00532
Energy Fuels 2016, 30, 5693−5704

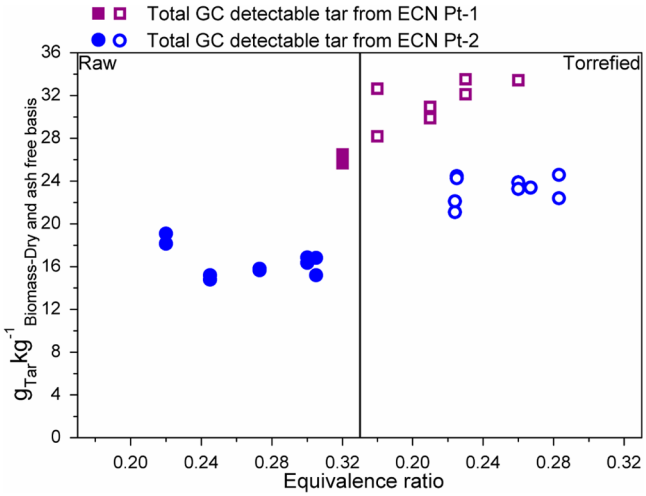


**Figure 7.** Equivalence ratio profile of the total GC-detectable tar at 800 °C operating temperature. Solid symbols, raw M×G; open symbols, torrefied M×G.

the following: (1) In the experimental rig, the gasification medium (i.e., air + $N_2$) was introduced below the distributor plate, whereas the biomass was introduced above the distributor plate. As mentioned earlier, devolatilization mainly occurred from the biomass particles floating on the top of the bed. Therefore, oxygen-driven tar cracking was limited because the oxygen introduced from the distributer plate is likely to have reacted with more reactive vapors[15] in the bed before reaching the freeboard where final tar formation took place. The residence time is short (<1 s) in the dense oxygen-rich phase, whereas it is longer in the freeboard with low oxygen levels (5−6 s). Longer residence time in the freeboard could overrule the effect of the ER. (2) Fresh uncalcined olivine was introduced into the reactor at the beginning of each day. A gasification temperature of 800 °C with local hot spots may have caused a gradual increase in olivine catalytic activity as the experiments progressed.[27] The catalytic activity of olivine was evaluated using the enrichment factor (EF) of the elutriated cyclone fines. According to Arena et al.[40] when olivine demonstrates significant catalytic activity for tar cracking, the fines collected in the cyclone contain substantially larger quantities of iron than those remaining in the reactor; consequently, the observed values of EF were significantly larger than 1. For the gasification experiments undertaken during the ECN Pt-2 campaign, the measured EFs for iron were in the range of 0.2−0.6, suggesting low or no catalytic activity from the elemental iron in olivine. However, according to Serrano et al.,[41] other elements present in olivine such as magnesium could have higher catalytic activity than iron. (3) More than one set of gasification conditions were tested within each day of experiments without discharging the bed between tests. Consequently, the char and ash that accumulated throughout the day may have offset ER in terms of the effect on tar evolution.[20]

Figure 7, which illustrates how total GC-detectable tar yield changes as a function of ER, shows that there is a significant difference between total GC-detectable tar observed for the two experimental campaigns. This cannot be explained by differences in chemical composition of the feedstocks, which came from the same batch of material and were within the margin of error. There was a notable difference in total GC-detectable tar yields (from 30 to 41%) between the first and second campaign (Figure 7) with corresponding ERs of 0.26 and 0.31. Such a deviation may have arisen from the operation and measurement inconsistencies between both campaigns. For example, the sampling efficiency of the SPA amino sorbent may have changed from one campaign to another, which in particular results in a poor sampling of secondary tars (such as benzene, toluene, and xylen). Notwithstanding potential inconsistencies and some discrepancies in operational conditions, the results nevertheless strongly suggest that the biomass composition plays a pivotal role in determining the yield of total GC-detectable tar.

The evolution of secondary, tertiary alkyl, and tertiary PAH tars as a function of ER is presented in Figure 8. The secondary

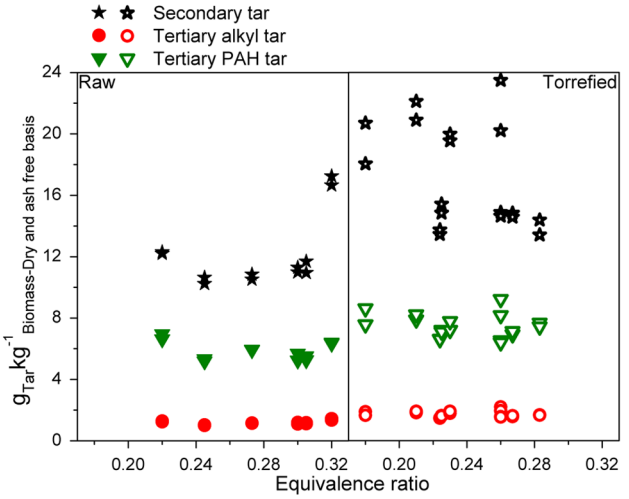


**Figure 8.** Equivalence ratio profile of the secondary, tertiary alkyl, and tertiary PAH tar group at 800 °C. Solid symbols, raw M×G; open symbols, torrefied M×G.

tars are the principal tar group over the range of ER investigated for both feedstock. Again, the yield of secondary tar species from torrefied M×G is higher than from raw biomass, which is related to the higher lignin content in the torrefied M×G as explained in section 3.1. However, tertiary PAH group is quantitatively close to the secondary tar group, and tertiary alkyl group remains the least significant which is in agreement with tar yields at 800 °C from the Figure 3.

The evolution of individual secondary tar compounds as a function of ER is presented in Figures 9a−f. The dominant tar compounds within this group are benzene, toluene, phenol, and indene, but the data points show no dependence on ER over the range studied. Kinoshita et al.[8] and Hanping et al.[16] however reported a decrease in phenol, xylene, and styrene over a similar ER range, whereas indene initially increased up to an ER of 0.25−0.27 and then decreased at higher ERs.

Figure 10a−f shows the evolution of individual tar compounds in the tertiary-alkyl and tertiary-PAH tar groups as a function of ER. Similar to the study of the temperature effect, 2-methyl-naphthalene is the most significant tertiary-alkyl tar compound with naphthalene, acenaphthylene, and phenanthrene being the most abundant compounds within the tertiary-PAH tar group for both biomasses. Torrefied M×G shows higher production of PAHs than raw M×G, but no definitive trend for the PAHs is observed over the ER range tested. However, the formation of PAHs at higher ER was reported by Kinoshita et al.[8] and Handing et al.,[16] suggesting that the PAHs production is stimulated at the higher ER.



DOI: 10.1021/acs.energyfuels.6b00532
*Energy Fuels* 2016, 30, 5693−5704

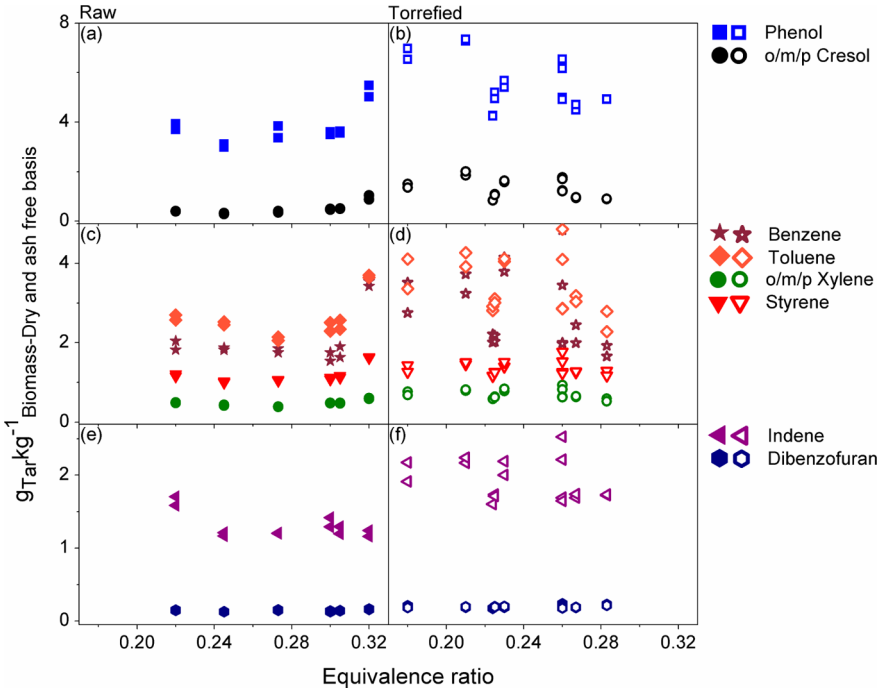


**Figure 9.** Equivalence ratio profile of the phenolic, single-ring aromatic, and two-ring aromatic tars from the secondary tar group at 800 °C. Solid symbols, raw M×G; open symbols, torrefied M×G.

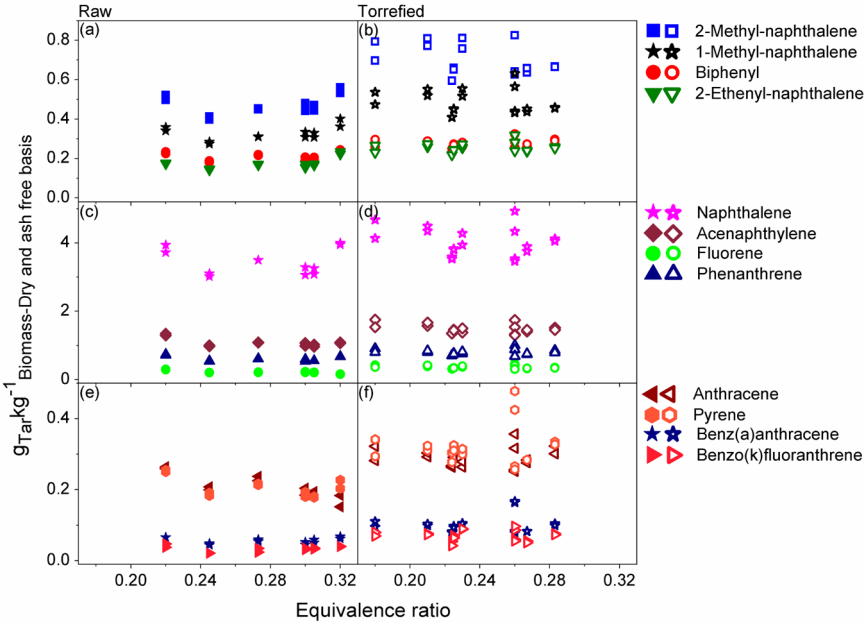


**Figure 10.** Equivalence ratio profile of the alkylated aromatic and PAH tars from the tertiary tar group at 800 °C. Solid symbols, raw M×G; open symbols, torrefied M×G.

## 4. CONCLUSIONS

Yields and composition of tar from the bubbling fluidized bed gasification of raw and torrefied M×G were investigated as a function of both temperature and equivalence ratio. For the range of gasification conditions tested, the following conclusions can be drawn: (1) The chemical composition of the feedstock is the most important parameter in determining tar evolution. There is an indication that torrefied M×G generates higher yields of both total GC-detectable tars as well as 20 individually quantified tar species. The total GC-detectable tar production from raw M×G is 14−19 $g_{\text{Total GC-detectable tar}}\ kg^{-1}_{\text{Biomass-daf}}$, whereas tar yield for torrefied M×G varies (21−31 $g_{\text{Total GC-detectable tar}}\ kg^{-1}_{\text{Biomass-daf}}$ measured for the temperature range). High tar content is attributed mainly to the higher lignin, but lower moisture content and the small particle size of the torrefied M×G may also contribute. (2) In terms of the effect of the operational conditions, temperature is demonstrated to play the dominant role in tar reforming reactions, namely, (a) tar cracking and (b) PAH enlarging. The highest yields of total GC-detectable tar, secondary tars, and tertiary-alkyl tars are typically observed between 700 and 800 °C, whereas tertiary polyaromatic



DOI: 10.1021/acs.energyfuels.6b00532
Energy Fuels 2016, 30, 5693−5704

tars increase up to the tested maximum temperature of 850 °C. Phenol is the most abundant species up to 800 °C, but at higher temperatures, naphthalene become dominant. The data from the two experimental campaigns suggests that at constant temperature the ER has relatively little impact on the amount or composition of tar.

## AUTHOR INFORMATION


### Corresponding Author

*E-mail: Marzena.Kwapinska@ul.ie.


### Notes

The authors declare no competing financial interest.

## ACKNOWLEDGMENTS

The financial support for this project provided by the EU project Biomass Research Infrastructure for Sharing Knowledge (BRISK) is gratefully acknowledged. We wish to thank the Energy Research Centre of Netherlands (ECN) for the technical support and cooperation. Special acknowledgement goes to Ben F. van Egmond for organizing access to the analytical laboratories, providing consumables, and sharing the knowledge. A.H. is supported by the Earth and Natural Sciences Doctoral Studies Programme which is funded by the Higher Education Authority (HEA) through the Programme for Research at Third Level Institutions, Cycle 5 (PRTLI-5) and is cofunded by the European Regional Development Fund (ERDF). M.K. is supported by the Enterprise Ireland Competence Centre for Biorefining & Biofuels (CC/2009/1305A) and INTERREG IVB NEW REsource Innovation Network for European Waste Project number 317J-RENEW. D.S.P. acknowledges funding from the People Programme (Marie Curie Actions) of the European Union's Seventh Framework Programme FP7/2007-2013/under REA grant agreement no [289887] and post-graduate research scholarship received from the University of Limerick, Ireland.

## REFERENCES


(1) Basu, P. *Biomass Gasification and Pyrolysis: Practical Design and Theory*; Academic press: Burlington, MA, 2010.

(2) *Biomass Gasification - Tar and Particles in Product Gases-Sampling and Analysis*; technical report P CEN/TS 15439; European Committee for Standardization: Brussels, 2006.

(3) Manyà, J. J.; Sánchez, J. L.; Gonzalo, A.; Arauzo, J. Air Gasification of Dried Sewage Sludge in a Fluidized Bed: Effect of the Operating Conditions and in-Bed Use of Alumina. *Energy Fuels* **2005**, *19*, 629−636.

(4) Berrueco, C.; Montané, D.; Matas Güell, B.; del Alamo, G. Effect of Temperature and Dolomite on Tar Formation during Gasification of Torrefied Biomass in a Pressurized Fluidized Bed. *Energy* **2014**, *66*, 849−859.

(5) Yu, H.; Zhang, Z.; Li, Z.; Chen, D. Characteristics of Tar Formation during Cellulose, Hemicellulose and Lignin Gasification. *Fuel* **2014**, *118*, 250−256.

(6) Narváez, I.; Orio, A.; Aznar, M. P.; Corella, J. Biomass Gasification with Air in an Atmospheric Bubbling Fluidized Bed. Effect of Six Operational Variables on the Quality of the Produced Raw Gas. *Ind. Eng. Chem. Res.* **1996**, *35*, 2110−2120.

(7) Milne, T. A.; Abatzoglou, N.; Evans, R. J. *Biomass Gasifier "Tars": Their Nature, Formation, and Conversion*; technical report NREL/TP-570-25357; National Renewable Energy Laboratory: Golden, CO, 1998; Vol. *570*.

(8) Kinoshita, C.; Wang, Y.; Zhou, J. Tar Formation under Different Biomass Gasification Conditions. *J. Anal. Appl. Pyrolysis* **1994**, *29*, 169−181.

(9) Van Paasen, S.; Kiel, J.; Veringa, H. *Tar Formation in a Fluidised Bed Gasifier: Impact of fuel properties and operating conditions.* Technical report ECN-C--04-013; Energy Research Centre of The Netherlands, Biomass: Petten, The Netherlands, 2004.

(10) Rabou, L. P.; Zwart, R. W.; Vreugdenhil, B. J.; Bos, L. Tar in Biomass Producer Gas, the Energy Research Centre of the Netherlands (ECN) Experience: An Enduring Challenge. *Energy Fuels* **2009**, *23*, 6189−6198.

(11) Jess, A. Mechanisms and Kinetics of Thermal Reactions of Aromatic Hydrocarbons from Pyrolysis of Solid Fuels. *Fuel* **1996**, *75*, 1441−1448.

(12) Morgan, T. J.; Kandiyoti, R. Pyrolysis of Coals and Biomass: Analysis of Thermal Breakdown and Its Products. *Chem. Rev.* **2014**, *114*, 1547−1607.

(13) Devi, L.; Ptasinski, K. J.; Janssen, F. J. A Review of the Primary Measures for Tar Elimination in Biomass Gasification Processes. *Biomass Bioenergy* **2003**, *24*, 125−140.

(14) Fitzpatrick, E.; Jones, J.; Pourkashanian, M.; Ross, A.; Williams, A.; Bartle, K. Mechanistic Aspects of Soot Formation from the Combustion of Pine Wood. *Energy Fuels* **2008**, *22*, 3771−3778.

(15) Gómez-Barea, A.; Ollero, P.; Leckner, B. Optimization of Char and Tar Conversion in Fluidized Bed Biomass Gasifiers. *Fuel* **2013**, *103*, 42−52.

(16) Hanping, C.; Bin, L.; Haiping, Y.; Guolai, Y.; Shihong, Z. Experimental Investigation of Biomass Gasification in a Fluidized Bed Reactor. *Energy Fuels* **2008**, *22*, 3493−3498.

(17) Link, S.; Arvelakis, S.; Paist, A.; Martin, A.; Liliedahl, T.; Sjöström, K. Atmospheric Fluidized Bed Gasification of Untreated and Leached Olive Residue, and Co-Gasification of Olive Residue, Reed, Pine Pellets and Douglas Fir Wood Chips. *Appl. Energy* **2012**, *94*, 89−97.

(18) Morgan, T. J.; Turn, S. Q.; Sun, N.; George, A. Fast Pyrolysis of Tropical Biomass Species and Influence of Water Pretreatment on Product Distributions. *PLoS One* **2016**, *11*, e0151368.

(19) Mayerhofer, M.; Fendt, S.; Spliethoff, H.; Gaderer, M. Fluidized Bed Gasification of Biomass-In Bed Investigation of Gas and Tar Formation. *Fuel* **2014**, *117*, 1248−1255.

(20) Abu El-Rub, Z.; Bramer, E.; Brem, G. Experimental Comparison of Biomass Chars with Other Catalysts for Tar Reduction. *Fuel* **2008**, *87*, 2243−2252.

(21) Chen, Q.; Zhou, J.; Liu, B.; Mei, Q.; Luo, Z. Influence of Torrefaction Pretreatment on Biomass Gasification Technology. *Chin. Sci. Bull.* **2011**, *56*, 1449−1456.

(22) Chen, W.-H.; Peng, J.; Bi, X. T. A State-of-the-Art Review of Biomass Torrefaction, Densification and Applications. *Renewable Sustainable Energy Rev.* **2015**, *44*, 847−866.

(23) Meng, J.; Park, J.; Tilotta, D.; Park, S. The Effect of Torrefaction on the Chemistry of Fast-Pyrolysis Bio-Oil. *Bioresour. Technol.* **2012**, *111*, 439−446.

(24) Boateng, A.; Mullen, C. Fast Pyrolysis of Biomass Thermally Pretreated by Torrefaction. *J. Anal. Appl. Pyrolysis* **2013**, *100*, 95−102.

(25) Corella, J.; Toledo, J. M.; Padilla, R. Olivine or Dolomite as in-Bed Additive in Biomass Gasification with Air in a Fluidized Bed: Which Is Better? *Energy Fuels* **2004**, *18*, 713−720.

(26) Rapagna, S.; Jand, N.; Kiennemann, A.; Foscolo, P. Steam-Gasification of Biomass in a Fluidised-Bed of Olivine Particles. *Biomass Bioenergy* **2000**, *19*, 187−197.

(27) Kuhn, J. N.; Zhao, Z.; Felix, L. G.; Slimane, R. B.; Choi, C. W.; Ozkan, U. S. Olivine Catalysts for Methane-and Tar-Steam Reforming. *Appl. Catal., B* **2008**, *81*, 14−26.

(28) Devi, L.; Ptasinski, K. J.; Janssen, F. J. Pretreated Olivine as Tar Removal Catalyst for Biomass Gasifiers: Investigation Using Naphthalene as Model Biomass Tar. *Fuel Process. Technol.* **2005**, *86*, 707−730.

(29) Abelha, P.; Franco, C.; Pinto, F.; Lopes, H.; Gulyurtlu, I.; Gominho, J.; Lourenço, A.; Pereira, H. Thermal Conversion of Cynara Cardunculus L. and Mixtures with Eucalyptus Globulus by Fluidized-Bed Combustion and Gasification. *Energy Fuels* **2013**, *27*, 6725−6737.

(30) Xue, G.; Kwapinska, M.; Horvat, A.; Kwapinski, W.; Rabou, L.; Dooley, S.; Czajka, K.; Leahy, J. Gasification of Torrefied Miscanthus_X Giganteus in an Air-Blown Bubbling Fluidized Bed Gasifier. *Bioresour. Technol.* **2014**, *159*, 397−403.




DOI: 10.1021/acs.energyfuels.6b00532
*Energy Fuels* 2016, 30, 5693−5704

(31) Kwapinska, M.; Xue, G.; Horvat, A.; Rabou, L. P.; Dooley, S.; Kwapinski, W.; Leahy, J. J. Fluidized Bed Gasification of Torrefied and Raw Grassy Biomass (Miscanthus X Gigantenus). The Effect of Operating Conditions on Process Performance. *Energy Fuels* **2015**, *29*, 7290−7300.
(32) Horvat, A.; Kwapinska, M.; Xue, G.; Dooley, S.; Kwapinski, W.; Leahy, J. J. Detailed Measurement Uncertainty Analysis of Solid-Phase Adsorption□ Total Gas Chromatography (GC)-Detectable Tar from Biomass Gasification. *Energy Fuels* **2016**, *30*, 2187−2197.
(33) Ortiz, I.; Pérez, R. M.; Sánchez, J. M. Evaluation of the Uncertainty Associated to Tar Sampling with Solid Phase Adsorption Cartridges. *Biomass Bioenergy* **2013**, *57*, 243−248.
(34) Israelsson, M.; Seemann, M.; Thunman, H. Assessment of the Solid-Phase Adsorption Method for Sampling Biomass-Derived Tar in Industrial Environments. *Energy Fuels* **2013**, *27*, 7569−7578.
(35) Kuo, J.-H.; Lian, Y.-H.; Rau, J.-Y.; Wey, M.-Y.; Lin, C.-L. Effect of Operating Conditions on Emission Concentration of PAHs during Fluidized Bed Air Gasification of Biomass. *Chemistry and Chemical Engineering (ICCCE), 2010 International Conference on* **2010**, 76−79.
(36) Padban, N.; Wang, W.; Ye, Z.; Bjerle, I.; Odenbrand, I. Tar Formation in Pressurized Fluidized Bed Air Gasification of Woody Biomass. *Energy Fuels* **2000**, *14*, 603−611.
(37) Dufour, A.; Masson, E.; Girods, P.; Rogaume, Y.; Zoulalian, A. Evolution of Aromatic Tar Composition in Relation to Methane and Ethylene from Biomass Pyrolysis-Gasification. *Energy Fuels* **2011**, *25*, 4182−4189.
(38) Ortiz González, I.; Pérez Pastor, R. M.; Sánchez Hervás, J. M. Sampling of Tar from Sewage Sludge Gasification Using Solid Phase Adsorption. *Anal. Bioanal. Chem.* **2012**, *403*, 2039−2046.
(39) Brage, C.; Yu, Q.; Sjöström, K. Characteristics of Evolution of Tar from Wood Pyrolysis in a Fixed-Bed Reactor. *Fuel* **1996**, *75*, 213−219.
(40) Arena, U.; Zaccariello, L.; Mastellone, M. L. Fluidized Bed Gasification of Waste-Derived Fuels. *Waste Manage.* **2010**, *30*, 1212−1219.
(41) Serrano, D.; Kwapinska, M.; Horvat, A.; Sánchez-Delgado, S.; Leahy, J. J. Cynara cardunculus L. Gasification in a Bubbling Fluidized Bed: The Effect of Magnesite and Olivine on Product Gas, Tar and Gasification Performance. *Fuel* **2016**, *173*, 247.



DOI: 10.1021/acs.energyfuels.6b00532
*Energy Fuels* 2016, 30, 5693−5704